

Development of a Polishing Robot System

Wang, Y.T. and Wang, C.P.

Dept. Mechanical Engineering, Tamkang University, 151 Ying-Chuan Rd., Tamsui, Taipei, Taiwan 25137
Taipei (Taiwan) T. +886 2 26205337 F. +886 2 26209745 E-mail: ytwang@mail.tku.edu.tw

Abstract - This paper presents the development of a robot-assisted surface finishing system with an active force controller. The system utilizes a dexterous manipulator to attain the desired position and orientation in three-dimensional space during finishing processes. This single-axis force controller consists of a DC motor and a software observer. The DC motor is attached to the robot wrist and used to actuate a pneumatic hand-grinder. The force observer is designed to sense the grinding contact-force based on the driving current and output position of the motor. The function of the active force controller includes observing the polishing contact force, applying a desired polishing pressure in the normal direction of the workpiece surface, and adjusting the contact angle between the hand-grinder and the surface of the workpiece. In this research, the prototype of a robot-assisted polishing system is constructed and tested on a Tatung A-530 robot. The experimental results show that the robot-assisted polishing system functions well under a variety of grinding and polishing conditions.

1. INTRODUCTION

Grinding and polishing processes are time-consuming and monotonous operations which strongly rely on skilled human-workers. To automate these processes and achieve desired surface finishing, it is important to control the grinding path, feed rate, grinding-wheel speed, contact force and cutting depth. Among them, the generation of a suitable tool-path and the control of contact forces are two major challenge issues. For example, to polish free-form surfaces of an object requires a delicate machine to follow complicated polishing paths. In this case, a polishing system based on a robot manipulator is more effective than that on a NC machining center in order to follow the curved free-form surfaces. On the other hand, during polishing operations, the tool comes into physical contact with the workpiece and causes contact forces between them. It is difficult to control these contact forces which depend on the cutting depth, feed rate, grinding-wheel speed and material properties.

Many researchers have proposed automated grinding and polishing systems for polishing of dies, deburring of castings and removing of weld beans etc [4-7,10]. Usually, a polishing tool is mounted on a NC machining center or a robot manipulator and a multi-dimensional force sensor is included in the system to improve finishing accuracy. It is troublesome to handle the multi-dimensional force control system in run-time processes, besides the passive-type force sensors are expensive in price and sensitive to a noise.

We propose an automated finishing system for polishing a free-form surface using an active force controller mounted on the wrist of an industrial robot. To simplify the force-control action, only the contact force normal to

the polishing surface is concerned and a software-type force observer is used to replace the role of a hardware sensor.

2. POLISHING ROBOT SYSTEM

The developed robot-assisted surface finishing system consists of an articulated industrial robot, an end-effector, a robot controller, a work table for setting a metal mold, a personal computer for sensory processing essential to a contact force control and a positioning work. The system configuration is shown as Figure 1. The system utilizes a dexterous manipulator to attain the desired position and orientation of the end-effector in three-dimensional space. A pneumatic hand-grinder is serially mounted on the end-effector. We control the motion and contact forces of the hand-grinder to perform the desired polishing action. The polishing robot follows a zigzag tool path and directs the hand-grinder to come in contact with the workpiece. The single-axis force observer can sense the contact force and drive the hand-grinder to apply a desired contact pressure on the workpiece. The force control algorithm of the observer with a hand-grinder is derived in the following section.

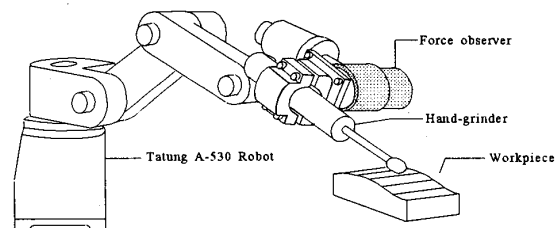


Figure 1 Polishing Robot System

3. FORCE CONTROL

In the force control system, only the normal contact pressure is concerned. The dynamic equation of the end-effector system with a hand-grinder can be expressed as

$$T_{em} = J\ddot{\theta} + k_e\theta + T_L \quad (1)$$

where T_{em} and T_L are the actuating and load torque, respectively. J is the inertia of the system; k_e is the contact compliance; $k_e\theta = T_f$ is the contact force with the workpiece. Equation (1) can be rewritten as the following equation with the new variable T_f

$$T_{em} = Jk_e^{-1}\ddot{T}_f + T_f + T_L \quad (2)$$

According to the concept of a partitioned controller [3], we can design a proportional-integral-derivative (PID) force controller

$$T_{em} = Jk_e^{-1}\left[\dot{T}^* + k_{fp}e_f + k_{fi}\int e_f dt + k_{fd}\dot{e}_f\right] + T_f + T_L \quad (3)$$

where T^* denotes the force command; e_f is the force error, $e_f = T^* - T_f$; k_{fp} , k_{fi} and k_{fd} are the gain values of the PID controller. In this case, T_L is not suitable to be put in the controller because it is not easy to be measured on-line. The term $(T_f + T_L)$ in Equation (3) is replaced by a feed-forward command T^* . The resultant controller is a PID-plus-feedforward (PIDFF) controller,

$$T_{em} = Jk_e^{-1}\left[\dot{T}^* + k_{fp}e_f + k_{fi}\int e_f dt + k_{fd}\dot{e}_f\right] + T^* \quad (4)$$

The block diagram of the PIDFF controller is shown as Figure 2. Where k_t is the torque constant of the motor; \hat{J} , \hat{k}_e and \hat{k}_t are the estimated values of the system parameters J , k_e and k_t , respectively. In the feedback loop, we replace sT_f by $k_e\omega$ in order to reduce the signal noise in the system. Where ω is the angular speed of the motor. In the finishing processes, the contact force will be kept at a constant value, i.e. $\dot{T}^* = \ddot{T}^* = 0$.

From Equation (2) and (4), we find the error equation,

$$\begin{aligned} \ddot{e}_f + k_{fd}\dot{e}_f + \frac{e_f}{Jk_e^{-1}} + k_{fi}\int e_f dt &= T_L \\ \ddot{e}_f + k_{fd}\dot{e}_f + k_{fp}\dot{e}_f + k_{fp}e_f + k_{fi}e_f &= \dot{T}_L \end{aligned}$$

We can see that the value of the steady-state error vanishes as time approaches infinity. If the estimated values of the system parameters are correct, we can

derive the transfer function which represents the relationship between the output force, T_f , and the input force and disturbance, T^* and T_L ,

$$\begin{aligned} \frac{Js^2}{k_e}T_f &= \left[\left(k_{fp} + \frac{k_{fi}}{s}\right)T^* - \left(k_{fp} + \frac{k_{fi}}{s} + k_{fd}s\right)T_f \right] Jk_e^{-1} + T^* - T_f - T_L \\ \frac{T_f}{T^*} &= \frac{(Jk_{fp} + k_e)s + Jk_{fi}}{Js^3 + Jk_{fd}s^2 + (Jk_{fp} + k_e)s + Jk_{fi}} \quad (5) \end{aligned}$$

In the case of no disturbance, the output will track the command exactly at the steady state. If there exists a disturbance, T_L , the steady-state error will disappear as time approaches infinity.

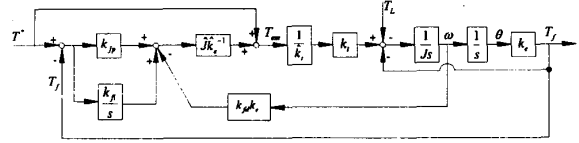


Figure 2 Block diagram of the PIDFF controller

The PIDFF controller provides a solution for the force control algorithm during the polishing process and the analytical and experiment works in this paper are based on the concept of the PIDFF controller.

4. Force Observer

We utilize a force observer to estimate the contact force during the finishing processes. The force observer is a linear Luenberger observer [8] as shown in Figure 3. The block diagram is composed of two parts: the upper loop is the motor system with a force controller and the lower one is the force observer. The force observer estimates the contact force based on the information of the torque command and the output position of the system.

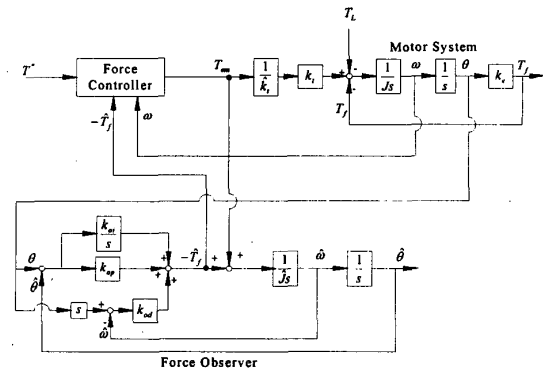


Figure 3 Force controller with a Luenberger observer

According to Figure 3, the observed torque can be determined as

$$\hat{T}_f = \frac{\hat{k}_t (k_{od}s^2 + k_{op}s + k_{oi})}{\hat{J}s^3 + k_{od}s^2 + k_{op}s + k_{oi}} T_f + \frac{\hat{J}(k_{od}s^3 + k_{op}s^2 + k_{oi}s)}{\hat{J}s^3 + k_{od}s^2 + k_{op}s + k_{oi}} \left[\left(\frac{\hat{J} \hat{k}_t}{\hat{J} \hat{k}_t} - 1 \right) \omega \right] \quad (6)$$

where k_{op} , k_{oi} and k_{od} are the gain values of the observer. If the parameters, \hat{k}_t and \hat{J} , are correctly estimated, Equation (6) can be simplified as

$$\frac{\hat{T}_f}{T_f} = \frac{(k_{od}s^2 + k_{op}s + k_{oi})}{\hat{J}s^3 + k_{od}s^2 + k_{op}s + k_{oi}} \quad (7)$$

In the steady state, the force observer can sense the contact force exactly. The transfer function of the PIDFF controller can be derived as follows.

$$\frac{Js^2}{k_e} T_f = \left[\left(k_{fp} + \frac{k_{fi}}{s} \right) T^* - \left(k_{fp} + \frac{k_{fi}}{s} + k_{fd}s \right) \hat{T}_f \right] \frac{J}{k_e} + T^* - T_f \quad (8)$$

Substituting Equation (7) into Equation (8), we have the transfer function,

$$\frac{T_f}{T^*} = \frac{n_4s^4 + n_3s^3 + n_2s^2 + n_1s + n_0}{d_6s^6 + d_5s^5 + d_4s^4 + d_3s^3 + d_2s^2 + d_1s + d_0} \quad (9)$$

Where

$$\begin{aligned} n_4 &= J^2 k_{fp} + Jk_e \\ n_3 &= J^2 k_{fi} + Jk_{fp}k_{od} + k_e k_{od} \\ n_2 &= Jk_{fi}k_{od} + Jk_{fp}k_{op} + k_e k_{op} \\ n_1 &= Jk_{fi}k_{op} + Jk_{fp}k_{oi} + k_e k_{oi} \\ n_0 &= Jk_{fi}k_{oi} \\ d_6 &= J^2 \\ d_5 &= Jk_{od} \\ d_4 &= Jk_e + Jk_{op} + Jk_{fd}k_{od} \\ d_3 &= k_{od}k_e + Jk_{oi} + Jk_{fd}k_{op} + Jk_{fp}k_{od} \\ d_2 &= k_{op}k_e + Jk_{fd}k_{oi} + Jk_{fp}k_{op} + Jk_{fi}k_{od} \\ d_1 &= k_e k_{oi} + Jk_{fp}k_{oi} + Jk_{fi}k_{op} \\ d_0 &= Jk_{fi}k_{oi} \end{aligned}$$

5. Force Observer Specification

The parameters of the DC observer-motor system are listed in Table 1. The controller is equipped with a PCL-726 D/A interface card and a PCL-833 encoder card by Advantech [1,2]. The D/A card has a 12-bits resolution to represent the output current in the range of $\pm 5A$. The basic unit of the current command of the motor drive is calculated as

$$10A \times \frac{1}{2^{12}} = \frac{10}{4095} \cong 2.44 \text{ mA}$$

The resolution of the force observer is

$$\begin{aligned} T &= i \times k_t = 2.44 \text{ mA} \times 0.185 \frac{\text{N} \cdot \text{m}}{\text{Amp}} \\ &= 0.4514 \text{ mN} \cdot \text{m} \times \frac{1 \text{ kgf}}{9.81 \text{ N}} \cong 4.601 \times 10^{-2} \text{ kgf} \cdot \text{mm} \end{aligned}$$

The distance between the motor axis and the polishing contact point is 95mm. Then, the resolution of the polishing pressure is

$$4.601 \times 10^{-2} / 95 \text{ mm} = 0.48 \text{ gf}$$

This is the smallest force can be applied by the active force controller. On the other hand, the maximum output-torque is limited by the rate-current of the motor which value is 1 ampere in this case. The maximum output torque can be generated by the force controller is determined as

$$T = 0.185 \frac{\text{N} \cdot \text{m}}{\text{Amp}} \times 1 \text{ Amp} \times \frac{1 \text{ kgf}}{9.81 \text{ N}} \times \frac{1000 \text{ mm}}{1 \text{ m}} \cong 18.9 \text{ kgf} \cdot \text{mm}$$

which is about 199 gf for this system.

Table 1 Parameters of the observer-motor

Rated Power	60Watt
Rated Voltage	75V
Rated Current	1.2A
Torque Constant	0.185N·m/A
Rotor Inertia	1.72656×10 ⁻³ kg·m ²
Weight	0.8kgf

6. Contact Force Observation

In a polishing process, if the actual motion path differs from the desired one, the contact force at the tip of the polishing tool would not agree with the desired contact force in the transient response. We can measure this deviation of contact forces by using the Luenberger force observer. The experimental setup is shown as Figure 4. The observer-motor tracks the surface horizontally and goes over a step-raise of 10mm in height. The horizontal motion is controlled by a PID

position-loop with a damping ratio of 1 and a natural frequency of 50rad/sec . That is,

$$\zeta=1, \quad \omega_n=50 \text{ rad/sec}$$

The gains of the PID controller can be determined as [9]

$$k_p = 0.6865; \quad k_i = 0.01144; \quad k_d = 13.7302$$

The contact compliance, k_e , of the metal probe in Figure 4 is 7.44Nm/rad . The observed contact force, T_{ob} , is shown in Figure 5. We can see that the step-rise of the tool-path will result in an increase of contact force.

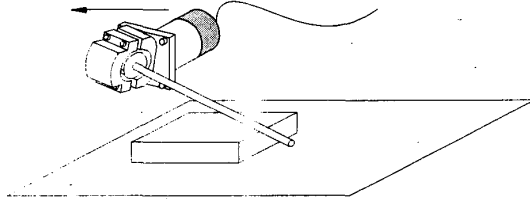


Figure 4 Physical setup of the force observer with a metal probe

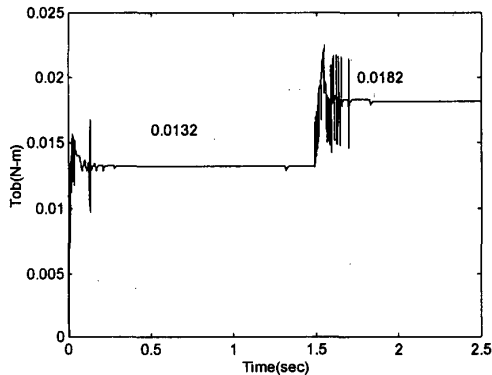


Figure 5 Observed force versus time

7. Polishing Force Control

In this example, we control the polishing robot to move in a straight-line path. The observer-motor with a pneumatic hand-grinder is equipped on the wrist of the robot. To simulate the deviation of polishing contour, we put a step-rise of 10mm in the straight-line path. The hand-grinder is driven to cross over the step-arise, while the contact force is retained at a constant value. We utilize the proposed PIDFF algorithm for the force-control system and a point-to-point motion-control algorithm for the robot system. The experimental setup is shown as Figure 4. The estimated inertia and contact compliance of the motor and metal-probe system are

$\hat{J}=0.0013\text{kgm}^2$ and $\hat{k}_e=7.44\text{Nm/rad}$, respectively. The gains of the force controller and observer are

$$k_{fp}=118.558; \quad k_{fi}=98716.9; \quad k_{fd}=77.0747$$

$$k_{op}=16.9582; \quad k_{oi}=326.523; \quad k_{od}=0.4212$$

The force-control action during a grinding process is simulated by using Matlab/Simulink, while the experimental work is tested on a Tatumg A530 robot. The simulation and experimental results are plotted in Figure 6, where the values of $\text{sim.}T_f$ and $\text{exp.}T_f$ denote the simulation and experimental forces, respectively. The grinding force is controlled at a fixed value of 0.12Nm .

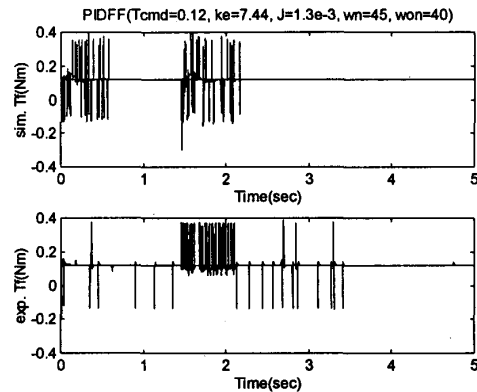


Figure 6 Simulation and experimental values of forces versus time

8. Polishing Robot System

The integrated polishing robot system is shown as Figure 7. The system includes a Tatumg A-530 robot for implementing the position and orientation of polishing processes. The force observer is a 60watt DC motor which is serial-connected to the wrist of the robot. The pneumatic hand-grinder is equipped at the front end of the force observer. The robot motion is controlled by a single-board controller. The estimated inertia and contact compliance of the hand-grinder system are

$$\hat{J} \cong 0.0011\text{kgm}^2$$

$$\hat{k}_e = 11.95 \text{ Nm / rad}$$

The gain values of the force controller and observer are given as

$$k_{fp}=299.3636; \quad k_{fi}=226981; \quad k_{fd}=183$$

$$k_{op}=5.28; \quad k_{oi}=70.4; \quad k_{od}=0.132$$

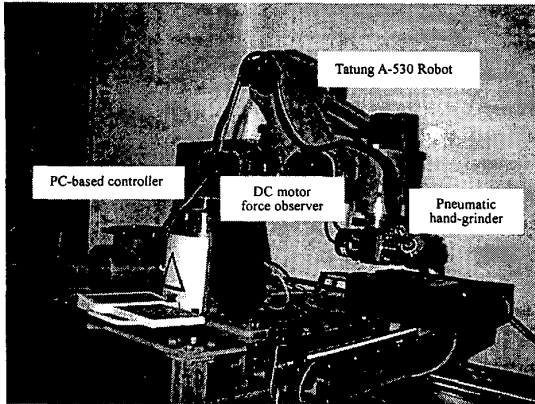


Figure 7 Automated Surface Finishing System

The experimental conditions are as follows: the workpiece is a stainless steel ST304 with a free-form surface; grinder-spindle rotation frequency is 5000rpm; applied contact torque is 0.12Nm; feed rate is 20mm/sec. The results are shown in Figure 8 and Figure 9. Figure 8 depicts the observed torque value and Figure 9 presents the ground workpiece. The results show that the system can track the free-form surface and retain a constant grinding force on the workpiece.

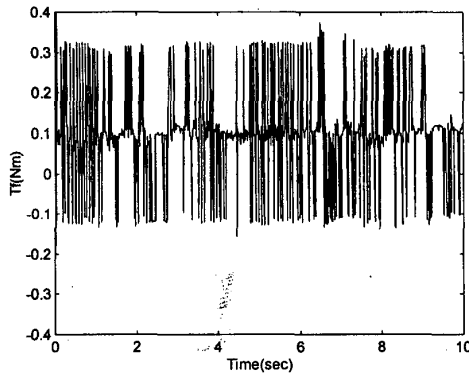


Figure 8 The observed grinding torque

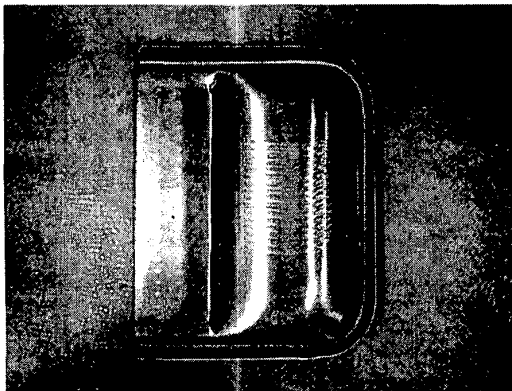


Figure 9 Ground curved-surface of a workpiece

9. Conclusions

This paper presents the development of a robot-assisted surface finishing system with an active force controller. This system utilizes a dexterous manipulator to attain the desired position and orientation of polishing processes in three-dimensional space. A force observer is attached to the tool frame of the robot manipulator, and a pneumatic hand-grinder is serially mounted on the observer. The function of the active force controller in the system includes observing the polishing contact force, applying a desired polishing pressure in the normal direction of workpiece surface, and adjusting the contact angle between the hand-grinder and the surface of the workpiece. In this research, we construct the prototype of a robot-assisted polishing system. The performance analysis and simulation of the force observer and force controller are accomplished by using SIMULINK. The software and hardware of the force control system are tested on a Tatung A-530 robot, and the integrated system is used to polish a workpiece with free-form surfaces. The experimental results show that the developed force observer and controller function well under a variety of grinding and polishing conditions. We conclude that the developed polishing robot system has the capability to polish workpieces with free-form surfaces.

Acknowledgement

This work was supported by the National Science Council in Taiwan under grant no. NSC87-2212-E-032-003.

References

- [1] Advantech, 1994a, PCL-726 six-channel D/A output card user's manual.
- [2] Advantech, 1994b, PCL-833 3-axis quadrature encoder and counter card user's manual.
- [3] Craig, J.J., 1989, Introduction to Robotics Mechanics and Control, 2nd Ed., pp.365-389.
- [4] Furukawa, T., D.C. Rye, M.W.M.G. Dissanayake, and A.J. Barratt, 1996, Automated polishing of an unknown three-dimensional surface, Robotics & Computer-Integrated Manufacturing, Vol.12, No.3, pp.261-270.
- [5] Jenkins, H.E. and T.R. Kurfess, 1996, Design of A Robust Controller for A Grinding System, IEEE Transactions on Control Systems Technology, Vol. 4, No.1, pp.40-48.
- [6] Kunieda, M., T. Nakagawa, and T. Higuchi, 1984, Development of a Polishing Robot for Free Form Surface, Proceedings of the 5th International Conference On Production Engineering, pp.265-270, Tokyo.
- [7] Kurfess, T.R., D.E. Whitney, and M.L. Brown, 1988, Verification of a dynamic grinding model, Journal of Dynamic systems, Measurement and Control, Vol.110, n4, pp.403-409.

- [8] Luenberger, D.G., 1971, An Introduction to Observers, IEEE Transactions on automatic control, Vol. AC-16, No. 6, pp.596-602.
- [9] Perdikaris, G.A. and K.V. VanPatten, 1982, Computer Schemes for Modeling, Tuning, and Control of DC Motor Drive Systems, Proceedings of the Power Electronics International Conference, pp.83-96.
- [10] Takeuchi, Y. and D.-F. Ge, 1992, Generation of polished-sculptured surfaces by advanced machining center-robot complex, Proceeding of the IEEE International Conference on Robotics and Automation, pp.1126-1131.